AD-A174 769 THE REFLECTANCE AND THERMAL RESPONSE OF GRAPHITE FIBRE REINFORCED EPOXY D..(U) MATERIALS RESEARCH LABS ASCOT VALE (AUSTRALIA) D R BRIGHTON AUG 86 MRL-R-1014&6495 1/1

UNCLASSIFIED F/G 11/4 NL

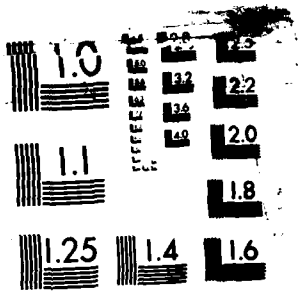

(12)

MRL-R-1014

AR-004-830

DEPARTMENT OF DEFENCE

DEFENCE SCIENCE AND TECHNOLOGY ORGANISATION

MATERIALS RESEARCH LABORATORIES

MELBOURNE, VICTORIA

REPORT

MRL-R-1014

THE REFLECTANCE AND THERMAL RESPONSE OF GRAPHITE FIBRE REINFORCED EPOXY DURING IRRADIATION BY A HIGH-POWER CO_2 LASER

David R. Brighton

Approved for Public Release

AUGUST 1986

DEPARTMENT OF DEFENCE
MATERIALS RESEARCH LABORATORIES

REPORT
MRL-R-1014

THE REFLECTANCE AND THERMAL RESPONSE OF GRAPHITE FIBRE REINFORCED EPOXY DURING IRRADIATION BY A HIGH-POWER CO_2 LASER

David R. Brighton

ABSTRACT

Graphite fibre reinforced epoxy (GFRP) samples were irradiated by a high-power CO_2 laser while the samples were exposed to high-speed flows of argon and air. Part of the angular distribution of the reflected CO_2 radiation was measured as a function of time and the total reflectance/absorptance estimated. The thermal response of the samples was measured using thermocouples embedded in the samples.

A one-dimensional model was used to show that one set of parameters could predict both the observed thermal response and the mass-loss rate that had been observed by other experimenters. The values of ablation enthalpy and absorptance derived from the model appear to be effective values that compensate for effects that are not included in the model, such as the mechanical removal of material and the combustion of decomposition products in air near the surface of the samples.

POSTAL ADDRESS: Director, Materials Research Laboratories
P.O. Box 50, Ascot Vale, Victoria 3032, Australia

SECURITY CLASSIFICATION OF THIS PAGE **UNCLASSIFIED**

DOCUMENT CONTROL DATA SHEET

REPORT NO.	AR NO.	REPORT SECURITY CLASSIFICATION
MRL-R-1014	AR-004-830	Unclassified

TITLE

The reflectance and thermal response of graphite fibre reinforced epoxy during irradiation by a high-power CO_2 laser

AUTHOR(S)

David R. Brighton

CORPORATE AUTHOR

Materials Research Laboratories
PO Box 50,
Ascot Vale, Victoria 3032

REPORT DATE	TASK NO.	SPONSOR
August 1986	DST 85/117	DSTO

FILE NO.	REFERENCES	PAGES
G6/4/8-3132	9	23

CLASSIFICATION/LIMITATION REVIEW DATE

CLASSIFICATION/RELEASE AUTHORITY
Superintendent, MRL
Physics Division

SECONDARY DISTRIBUTION

Approved for Public Release

ANNOUNCEMENT

Announcement of this report is unlimited

KEYWORDS

Graphite Composites
Graphite Fibre Reinforced Epoxies
Laser Irradiation
Thermal Response
Reflectance

COSATI GROUPS 2005

ABSTRACT

Graphite fibre reinforced epoxy (GFRP) samples were irradiated by a high-power CO_2 laser while the samples were exposed to high-speed flows of argon and air. Part of the angular distribution of the reflected CO_2 radiation was measured as a function of time and the total reflectance/absorptance estimated. The thermal response of the samples was measured using thermocouples embedded in the samples.

A one-dimensional model was used to show that one set of parameters could predict both the observed thermal response and the mass-loss rate that had been observed by other experimenters. The values of ablation enthalpy and absorptance derived from the model appear to be effective values that compensate for effects that are not included in the model, such as the mechanical removal of material and the combustion of decomposition products in air near the surface of the samples.

CONTENTS

THE REFLECTANCE AND THERMAL RESPONSE OF GRAPHITE FIBRE REINFORCED EPOXY DURING IRRADIATION BY A HIGH-POWER CO_2 LASER

1. INTRODUCTION

Graphite fibre reinforced epoxy or plastic (GFRP) materials are increasingly being used for military applications, in particular in aircraft because of the high strength-to-weight ratio of these composite materials. However, due to the rapid degradation of the composite's mechanical properties at temperatures above about 500 K [1], high-power laser radiation may pose a threat to the structural integrity of load-bearing members constructed from such composite materials [2]. Accurate modelling of the composite's thermal response is an important part in assessing the threat posed to composite structures by high-power lasers.

Griffis, Masumura and Chang [3] used a one-dimensional model to analyse the thermal response of AS/3501-6 (Hercules Corp.) graphite-epoxy laminate to high-power laser radiation. The present study describes thermal response measurements made on a similar GFRP material and an analysis using the same one-dimensional model. The target reflectance, which controls the thermal coupling to the target, is an important parameter in the model and this parameter has been measured as a function of the laser irradiation time. The model does not take into account the mechanical removal of target material by an airstream, nor does it take into account the energy generated by combustion processes. These effects are shown to be important and point to the need to use effective values of parameters in the model, rather than values that have a strict physical interpretation.

2. EXPERIMENTAL DETAILS

2.1 Laser Facility

The laser facility [4,5] and the experimental arrangement [6] have been described previously. Briefly, the facility comprises a 20 kW continuous-wave CO_2 laser, the beam from which was manipulated to obtain near-uniform irradiation on a target area of either 9 mm x 9 mm or 17 mm x 17 mm. Each target sample was located flush with the wall of a wind tunnel, the wind direction being perpendicular to the incident beam. Wind speeds of about M = 0.85 were employed.

2.2 Target Samples

Target samples were prepared from a graphite fibre prepreg commonly known as "DDS/828/carbon composite". The details of the prepreg material are as follows:

Cloth - Woven rovings, Fothergill and Harvey style A004, 0.283 kg m^{-2}, 0.3 mm thick, 5 H satin weave 7 x 7 per cm in 3000 filament Toray carbon fibre.

Resin - 100 parts EPON 828 epoxy (Shell)
33 parts Diaminodiphenyl sulphone (DDS)

Resin content - 33 ± 2% to give 60% fibre volume in cured composite.

The prepreg was cured at a temperature of 390 K under a pressure of 550 kPa for 24 hours. After curing, each ply was nominally 0.25 mm thick.

Target samples for the thermal response measurements were prepared by incorporating thermocouples into 8-ply samples. Chromel-alumel thermocouples (0.07 mm diameter) were tucked partly into the weave of the material to prevent the thermocouple becoming detached when the epoxy vaporised. The 8-ply samples generally had thermocouples embedded every second ply in a position near the beam axis. Arbitrarily defining one of the directions along the weave as 0°, the 8-ply samples were laid up employing the sequence of 0°, 45°, 45°, 0°, 0°, 45°, 45°, 0°.

Target samples for the reflectance measurements comprised 8 plies, layed-up in the same sequence as above, but without any thermocouples.

2.3 Detector Array

To determine the reflectance of a target sample, laser radiation reflected from the sample was detected by an array of 9 black, anodized aluminium plates located on the side of the wind tunnel opposite the target. Both the plates and the target were vertical and the distance between the plane of the array and the target surface was 77 mm. Each plate

had the dimensions 8 mm x 4 mm x 0.4 mm with an average mass of 0.033 g. Three plates were placed upwind (designated P1, P2 and P3) and six downwind (designated P4 to P9 respectively) of the laser beam axis. The axis of the laser beam intersected the centre of the target and a horizontal plane through the beam axis intersected the centre of each plate. Each plate was centred 7 mm from its nearest neighbour, so that an angular range of 13^{o}–37^{o} from the sample normal was covered on the downwind side and 13^{o}–25^{o} on the upwind side. Fine-gauge chromel-alumel thermocouples (0.07 mm diameter) were spot welded to the rear face of the plates so that the temperature rise could be monitored.

To reduce the amount of blackbody radiation detected by the plates, a thin-film filter was fabricated and placed in front of the array. The filter transmitted 10.6 μm wavelength radiation, but rejected radiation with a wavelength near 1 μm, the region which corresponded to the peak of the blackbody radiation from a target with a surface temperature of approximately 3800 K. It was calculated that, with the filter in place, each plate would detect about 3.0 W m^{-2} from a blackbody source at 3800 K (assuming a diffusely-emitting surface with an emissivity of 1).

2.4 Data Logging

A microprocessor-based data logging system was used to record thermocouple and other detector responses. The system also controlled the duration of the laser irradiation pulse. The duration of the laser pulse was determined by monitoring the output from a fast Hg-Cd-Te detector (Infrared Associates Inc; Model No. HCT-55). The wind speed was calculated from measurements taken by a pressure transducer inserted in the wall of the wind tunnel. The front-surface temperature of the target was measured by an optical pyrometer operating at 0.9 μm (Ircon Model 720). The thermocouple outputs were logged after amplification. Each of these instruments was typically sampled every 4 ms for up to 3.2 seconds.

A beam splitter was used to reflect a known fraction of the incident energy on to a calorimeter. The cooling rate of the calorimeter was monitored for up to 30 seconds and used to estimate the laser energy incident on the calorimeter and, hence, the laser energy incident on the target.

3. EXPERIMENTAL RESULTS

3.1 Reflectance and Emittance of GFRP

3.1.1 Reflectance under High-Power CO_2 Laser Irradiation

The reflectance of another material was measured previously [6] with the present experimental arrangement. The response from the detector array as a function of laser irradiation time indicated that a correction was required for a small amount of laser radiation that was being reflected from the target holder onto the array. Allowance was made for this radiation, the amount of which varied according to the location of the array plate, but which did not exceed 8% of the radiation reflected from the target.

After the irradiation ceased, the cooling rate for a particular detector plate was used to estimate the heat loss from that plate during the laser irradiation and a corrected curve of plate temperature versus time was generated. Each curve was then multiplied by the thermal capacity of the plate and differentiated to give the power absorbed by the plate as a function of time. The thin plates were designed with a small thermal response time so that the rate of change of the rear-surface temperature corresponded to the power absorbed by the plate.

The front-surface temperature of the target was determined (section 3.2.1) assuming an emissivity of 0.85 [2] and an estimate was made of the amount of black-body radiation reaching the plate through the filter. Typically, the black-body radiation transmitted through the filter comprised about 25% of the total power absorbed by the plate and a correction was made for this radiation. This correction was proportionately larger than the correction required in a previous experiment [6], due to the higher target temperatures and lower target reflectances in this experiment.

For each plate, the absorbed power was normalised to indicate the directional reflectance, $\rho(\theta)$, as a function of time, i.e. the power per steradian reflected in the direction θ per unit incident power, where θ is the angle between the laser beam axis and the line from the target centre to the detector plate centre. The results for one graphite-epoxy composite sample irradiated at 60 MW m^{-2} are shown in fig. 1.

To estimate the total power reflected from the target, firstly, it was assumed that the angular distribution of the reflected power (W sr^{-1}) in a horizontal plane passing through the detector array could be described by the function

$$I(\theta) = A \cos\theta + B (1 - \sin\theta)^n \qquad (1)$$

That is, the reflected power was divided into two components - a diffusely reflected component, described as is usual by the cos θ term, and a non-diffusely reflected component, described conveniently by the $(1 - \sin\theta)^n$ term, where n is an index controlling how sharply peaked the distribution is. The second term has no physical interpretation, but was used for reasons discussed previously [6].

Then for each experimental run, values of A, B and n were obtained that gave reasonable fits to the reflected power distribution measured by the array of plates. The total power reflected from the target was estimated by integration of equation 1, assuming azimuthal symmetry, so that

$$\rho_{2\pi} = \int_0^{2\pi} \int_0^{\pi/2} [A \cos\theta + B (1 - \sin\theta)^n] \sin\theta \; d\theta \, d\phi \qquad (2)$$

where $\rho_{2\pi}$ is the total hemispherical reflectance, i.e. the fraction of the incident power, Φ, reflected into the solid angle 2π, and ϕ is the azimuthal angle. Fig. 2 shows values of $\rho_{2\pi}$, as a function of laser irradiation time for four GFRP samples exposed to incident power densities between 21 and 63 MW m^{-2}. Also listed are values of $\bar{\rho}_{2\pi}$, the total hemispherical reflectance averaged over the run time.

The parameters A and B in equation 1 were normalised by dividing by the product $\rho_{2\pi}\Phi$ to give normalised parameters a and b, such that

$$I(\theta) = \rho_{2\pi}\Phi [a \cos\theta + b(1-\sin\theta)^n] \qquad (3)$$

Table 1 shows the values of a, b and n obtained at various times during the irradiation of GFRP samples at irradiances between 21 and 63 MW m^{-2}.

As the reflected power had been divided into two components (equations 1 & 3), the total hemispherical reflectance, $\rho_{2\pi}$, was correspondingly divided into a diffuse component, ρ_d, and a non-diffuse component, ρ_{nd}, i.e.

$$\rho_{2\pi} = \rho_d + \rho_{nd} \qquad (4)$$

The values for the two components were obtained by separately integrating the two terms on the right-hand side of equation 3. These values are also shown in table 1.

As described in the paragraphs above, equation 1 has been used to extrapolate the angular distribution of the reflected power to regions where data were not available. Naturally, the magnitude of the reflectance estimated by integrating the angular distribution (equation 2) must be influenced by the lack of data in certain angular ranges. However, it is argued that data were taken over a sufficient angular range for the effect of the missing data to be small. It has been shown previously that such an extrapolation is reliable [6].

3.1.2 Reflectance under Low-Power CO_2 Laser Irradiation

A separate experiment was set up to determine the reflectance of a previously irradiated GFRP sample at ambient temperatures so that a comparison could be made with the reflectance derived under high-power irradiation. The

sample was placed on the axis of a goniometer and irradiated at nearly-normal incidence by a 1-W CO_2 laser with a beam stopped down to a diameter of 3 mm. A thermopile detector, located on the circumference of the goniometer, rotated about the axis and in the plane of the beam. This detector was used to measure the relative angular distribution of the reflected power for almost the complete angular range between 0^o and 90^o.

Measurements were made for the GFRP sample and also for a sand-blasted aluminium sample. The relative reflected power distributions were fitted using equation 1 and integrated according to equation 2. In addition, the absorptance (at 10.6 μm) of the sand-blasted aluminium samples was determined calorimetrically. From this measurement, the total hemispherical reflectance (at 10.6 μm) of the aluminium samples was known and the relative results obtained using the GFRP sample were normalised to absolute values. (The GFRP sample was too thick to allow accurate application of the calorimetric method.) The values of a, b and n obtained are shown in table 2, together with the corresponding calculated values of $\rho_{2\pi}$, ρ_d and ρ_{nd}, using the nomenclature of section 3.1.1. In section 4.2, the values of reflectance obtained under low-power irradiation (table 2) are compared with the values of reflectance obtained under high-power laser irradiation (table 1).

3.1.3 Emittance at 5 μm

Another separate experiment was set up to measure the emittance at 5 μm (and, by implication, the reflectance) of GFRP samples at near-ambient temperatures. These results were used to estimate the reflectance at 10.6 μm and hence to provide an independent check on the reflectance values obtained in the previous section.

A chromel-alumel thermocouple was attached by colloidal silver adhesive to the surface of a particular sample. The sample was heated to temperatures between 370 and 620 K and its apparent temperature measured by an Ircon pyrometer operating at 5 μm. Comparison of the apparent temperature observed by the pyrometer and the temperature determined by the thermocouple enabled the emittance of the sample to be deduced. The values deduced are shown in table 3.

The emittance values obtained at a wavelength of 5 μm (ε_5) were used to estimate emittance values, and hence reflectance values at 10.6 μm ($\rho_{10.6}$). From the literature, it was observed that the normal spectral emittance of various samples of graphite at 300 K scaled as approximately $\lambda^{-0.5}$ for wavelengths greater than about 5 μm [5]. On this basis, it was assumed that the spectral emittance of GFRP composite material would also scale approximately as $\lambda^{-0.5}$ and hence that

$$\rho_{10.6} \simeq 1 - \varepsilon_5 \left(\frac{5}{10.6}\right)^{0.5} \qquad (5)$$

The estimated reflectances, $\rho_{10.6}$, for a previously irradiated GFRP sample and for the woven graphite fibre reinforcing material (no epoxy) is shown in table 3 together with the value of reflectance, $\rho_{2\pi}$, obtained by integration (table 2). The two estimates are in good agreement.

3.2 Thermal Response of GFRP Epoxy under High-Power CO_2 Laser Irradiation

3.2.1 Surface Temperatures

During the high-power CO_2 laser irradiation, the surface temperature of each GFRP sample was monitored by an Ircon Modline II pyrometer operating at 0.9 μm. It was assumed that the emittance of the GFRP was 0.85 [7], and the corresponding temperatures are shown as a function of time in Fig. 3 for samples irradiated at 21, 30 and 63 MW m^{-2}. A variation of 0.01 in the assumed emissivity changes the predicted temperature by 10^{o}.

3.2.2 Internal Temperatures

Thermocouples placed in the samples measured internal temperatures of up to about 1600K. Thermocouples were located in every second ply of 8-ply GFRP samples. Fig. 4 shows how the temperature varied as a function of time for each location in one sample. The target was irradiated at a power density of 21.3 MW m^{-2} for 3.2 s in an air flow of M = 0.8. Fig. 5 shows an equivalent distribution for a target irradiated at a power density of 17.2 MW m^{-2} for 3.2 s, but in an argon atmosphere with M = 0.6.

4. THERMAL RESPONSE CALCULATIONS

Griffis, Masumura and Chang [3] developed a one-dimensional finite difference code to model the transient thermal response of laser-irradiated composite material samples. This code was used to calculate the mass loss and the temperature increase induced by laser irradiation. The thermophysical properties of the composite material used in the experiments reported here, DDS/828/carbon composite, were assumed to be the same as those used by Kennett for AS/3501-6 GFRP in other calculations [8].

Two parameters in the code, the absorption and the ablation enthalpy, were varied so that the mass-loss rate obtained by Kennett and McLachlan [9] for AS/3501-6 GFRP could be predicted. The predicted mass-loss rate, both in air and in argon, is shown in fig. 6 as a function of incident laser intensity together with the experimental data [9]. Good agreement was obtained using an absorptance of 0.9 in air and 0.8 in argon. An ablation enthalpy of 34.4 MJ kg^{-1} was used in both cases, which is 80% of that used by Griffis, Masumura and Chang [3]. The mass-loss rate in air was calculated assuming that there was no air flow across the surface of the target (M = 0). The significance of this and the other parameter values obtained is discussed in section 5.

These parameters were then used to predict the thermal response of 8-ply DDS/828/carbon composite samples at a power density of 21.3 MW m^{-2} in air and 17.2 MW m^{-2} in argon. The predictions are shown in figs. 4 and 5 together with the experimental data. The agreement is generally good, both at high temperatures, for thermocouples placed near the front surface of the

target, and at long irradiation times, for thermocouples placed near the back surface of the target.

5. DISCUSSION AND CONCLUSIONS

Part of the angular distribution of CO_2 laser radiation reflected from DDS/828/carbon composite material was measured while the material was subjected to high-power laser irradiation. The angular distribution was shown to vary in shape and magnitude with irradiation time. At the start of the irradiation, the angular distribution was more sharply peaked about the normal to the target surface than later in the irradiation (table 1). The maximum reflectance was observed between 0.3 and 0.6 s after the onset of irradiation (fig. 2). The reflected radiation was divided into a diffusely reflected component and a non-diffusely reflected component. However, no consistent trend could be discerned in the two components (table 1).

The reflectance and absorptance of GFRP at 10.6 μm have been estimated in a number of ways. These reflectance and absorptance coefficients are listed in table 4. From these results a number of points are apparent:

(i) The absorptance estimated from the 5 μm emittance measurement (0.65) is in reasonable agreement with the absorptance (0.60) estimated from the low-power irradiation.

(ii) The absorptance of the woven graphite fibre reinforcing material without epoxy (0.62) is similar to that of a previously irradiated target (0.65) indicating, as would be expected, that it is the graphite fibres that control the absorptance.

(iii) The absorptance at high temperatures, i.e. under high-power irradiation (0.69) is greater than the absorptance near room temperature, i.e. under low-power irradiation (0.60).

(iv) The absorptance used in the 1-D calculation for thermal response in air (0.9) is greater than that for thermal response in argon (0.8) and both absorptances are greater than the absorptance derived from the reflectance measurements (0.69).

It is apparent that the three absorptances mentioned in point (iv) above do not agree with each other. Some possible reasons for this may be seen by inspecting the expression for the steady-state mass loss predicted by the 1-D model for ablation of a semi-infinite target [3],

$$\dot{m} = \frac{\alpha I_o - I_r - I_c}{H + C\Delta T} \qquad (6)$$

where $\dot{m}$ is the mass-loss rate, α is the absorptance, I_o is the incident laser intensity, I_r and I_c represent the power losses due to radiation and convection respectively, H is the ablation enthalpy, C is the specific heat

and ΔT is the temperature difference between ambient and the ablation temperature.

The model does not take account of the possible contribution due to the combustion of decomposition products near the target surface. Combustion might be expected to take place for ablation in air, but not for ablation in argon. If the contribution of combustion to the mass-loss rate is partly dependent on the laser intensity, say βI_o, and partly independent of the laser intensity, say I_{com}, then the mass-loss rate may be written as

$$\dot{m} = \frac{\alpha I_o - I_r - I_c + \beta I_o + I_{com}}{H + C\Delta T} \qquad (7)$$

This implies that the effect of combustion can be simulated in the model by increasing the absorptance, i.e. using an effective absorptance $\alpha' = \alpha+\beta$, and by decreasing the loss term.

In fact, it was required to do this to get the model to predict the observed mass-loss rate in air. From this it may be concluded that if $\alpha' = 0.90$ (in air) and $\alpha = 0.80$ (in argon) then $\beta = 0.10$. In addition, it was required to ignore the convective losses ($M = 0$, section 4). This implies that $I_{com} \simeq I_c$, i.e. in this particular case the combustion effects compensate for the convective losses. The effective absorptance in air, 0.90, was similar to the value, 0.92, used by Griffis, Masumura and Chang [3].

Another factor that the model does not take account of is the mechanical removal of material by the airstream. The sudden decreases occasionally observed in the front surface temperature of targets (fig. 3) are thought to be caused by the mechanical removal of material. Consequently, the ablation enthalpy used in the model will be an effective value that is less than the actual value. The thermal response data used in this report were mainly obtained in gas flows with $M \simeq 0.8$, where mechanical removal is expected to be a more important mechanism than in the lower-velocity gas flows, $M \simeq 0.3$, used by Griffis, Masumura and Chang [3]. Thus, it is not surprising that a lower value of ablation enthalpy, 34.4 MJ kg^{-1}, was required to fit the thermal response data used in this report compared to the ablation enthalpy, 43 MJ kg^{-1}, used by Griffis, Masumura and Chang [3].

Returning to a discussion of the absorptance, the absorptance in argon derived from the mass-loss rate (0.8) is greater than the absorptance derived from the reflectance measurement (0.69). It was expected that the two estimates would agree more closely because the absorptance in argon was expected to represent the physical absorptance of the target assuming that there was no contribution from combustion products. One explanation of the discrepancy is apparent from an inspection of equation 6. The same mass-loss rate could be predicted using a smaller value of absorptance if the absorptance, the loss term and the enthalpy term were all correspondingly reduced. To bring the absorptance estimates into agreement would require a reduction of about 15% in all three quantities. An alternative explanation is that the target reflectance has been overestimated, and the target absorptance underestimated, due to the relatively large correction that was made for blackbody radiation. The relatively large size of this correction means that

the estimated absorptance is more sensitive to the assumptions made in calculating the correction.

As there is no strong reason to select one of the explanations given above at the expense of the other, the best estimate of the physical absorptance of the target is simply obtained by averaging the estimate from the mass-loss rate (0.8) and the estimate from the reflectance measurements (0.69) to give $\alpha = 0.75 \pm 0.05$.

In conclusion, the one-dimensional model of Griffis, Masumura and Chang [3] is able to predict with reasonable accuracy both the mass-loss rate of laser-irradiated GFRP samples and the temperature profiles within the samples. But, to do so realistically, it is necessary to use effective values of two of the model's parameters, the ablation enthalpy and the absorptance, in order to compensate for two effects that are not included in the model, the mechanical removal of material and the combustion of decomposition products in air near the surface of the samples.

6. ACKNOWLEDGEMENTS

The author wishes to thankfully acknowledge the technical assistance given by Mr E.J. Boere and Mr P.W. Dixon in setting up and running the experiment. The low-power reflectance measurements were made by Dr R.L. Calvert and the author is grateful for his help.

7. REFERENCES

1. Pering, G.A., Farrell, P.V. and Springer, G.S. (1980). "Degradation of Tensile and Shear Properties of Composites Exposed to Fire or High Temperature", J. Composite Materials 14, 54.

2. Kibler, K.G., Carter, H.G. and Eisenmann, J.R. (1977). "Response of Graphite Composites to Laser Irradiation", TR-77-0706, Air Force Office of Scientific Research (Bolling Air Force Base, Washington DC).

3. Griffis, C.A., Masumura, R.A. and Chang, C.I. (1981). "Thermal Response of Graphite Epoxy Composite Subjected to Rapid Heating", J. Composite Materials 15, 427.

4. McLeary, R.C., Whitcher, R.E. and Beckwith, P.J. (1979). "A 30-kW CO_2 Mixing Laser", Report MRL-R-751, Materials Research Laboratories, Melbourne, Victoria.

5. Crane, K.C.A., Garnsworthy, R.K. and Mathias, L.E.S. (1980). "Ablation of Materials Subjected to Laser Radiation and High-Speed Gas Flows", J. Appl. Phys. 51, 2954.

6. Brighton, D.R. and Gaylor, K. (1984). "The Reflectance of a TBR Composite Material During Irradiation by a High-Power CO_2 Laser", Report MRL-R-927, Materials Research Laboratories, Melbourne, Victoria.

7. Brown, J.R., Gellert, E.P. and Hilton, P.R. (1982). "Study of CW Laser-Induced Ablation of Composite Barrier Materials", Report MRL-R-840, Materials Research Laboratories, Melbourne, Victoria.

8. Kennett, S.R. (1985). "Thermal Response of Laser Irradiated Graphite-Fibre Reinforced Epoxies", Report MRL-R-961, Materials Research Laboratories, Melbourne, Victoria.

9. Kennett, S.R. and McLachlan, A.D. (1984). "Thermal Flux from the Decomposition Products of Laser-Irradiated Graphite-Epoxy Composite", Report MRL-R-926, Materials Research Laboratories, Melbourne, Victoria.

TABLE 1

Reflectance of GFRP Material Under High-Power CO_2 Laser Irradiation

Sample	Incident Power Density MW m^{-2}	Time s	a sr^{-1}	b sr^{-1}	n	$\rho_{2\pi}$	ρ_d	ρ_{nd}
GFRP 1	21	0.1	0.214	2.96	6	0.22	0.15	0.07
		0.2	0.214	2.96	6	0.22	0.15	0.07
		0.3	0.122	2.83	4	0.23	0.09	0.14
		0.4	0.162	2.24	4	0.29	0.15	0.14
		0.5	0.197	1.12	3	0.33	0.20	0.13
		0.7	0.240	0.66	3	0.35	0.26	0.09
		0.9	0.255	0.58	3	0.33	0.27	0.06
GFRP 2	30	0.2	0.197	1.08	3	0.36	0.22	0.14
		0.4	0.187	1.17	3	0.30	0.18	0.12
		0.6	0.202	0.26	1	0.42	0.27	0.15
		0.8	0.125	0.46	1	0.28	0.11	0.17
		1.0	0.097	0.52	1	0.29	0.09	0.20
		1.2	0.052	0.63	1	0.27	0.05	0.22
GFRP 3	60	0.08	0.215	1.00	3	0.27	0.18	0.09
		0.2	0.215	1.00	3	0.27	0.18	0.09
		0.3	0.274	0.23	2	0.42	0.36	0.06
		0.4	0.274	0.23	2	0.42	0.36	0.06
		0.5	0.216	0.25	1	0.31	0.21	0.10
		0.7	0.192	0.31	1	0.25	0.15	0.10
		0.9	0.192	0.31	1	0.25	0.15	0.10
GFRP 4	63	0.08	0.150	2.41	4	0.22	0.10	0.12
		0.2	0.289	0.29	3	0.35	0.31	0.04
		0.3	0.286	0.15	2	0.49	0.44	0.05
		0.4	0.276	0.22	2	0.38	0.33	0.05
		0.5	0.283	0.17	2	0.30	0.27	0.03

TABLE 2

Reflectance of GFRP Material Under Low-Power CO_2 Laser Irradiation

Sample	Incident Power Density* MW m^{-2}	a sr^{-1}	b sr^{-1}	n	$\rho_{2\pi}$	ρ_d	ρ_{nd}
GFRP 3	60	0.067	0.588	1	0.40	0.08	0.32
Aluminium (sand blasted)	unirradiated	0.240	0.183	1	0.78	0.59	0.19

* During previous irradiation

TABLE 3

Emittance and Reflectance of GFRP Material at 5 μm

Sample	ε_5	$\rho_{10.6}$	$\rho_{2\pi}$
GFRP 3[1]	0.93 ± 0.05	0.35	0.40
GFRP 5[2]	0.88 ± 0.10	0.38	

[1] Previously irradiated (60 MW m^{-2}) GFRP material.

[2] Woven graphite fibre reinforcing material.

TABLE 4

Reflectance and Absorptance of GFRP Material at 10.6 μm

Sample	Reflectance at 10.6 μm $\rho_{2\pi}$	Absorptance at 10.6 μm α
High-Power Irradiation		
- Time Averaged	0.31	0.69
Low-Power Irradiation		
- Previously Irradiated	0.40	0.60
Extrapolation from 5 μm Emittance		
- Previously Irradiated	0.35	0.65
- Woven Rovings Only	0.38	0.62
Values Used in Calculations		
- In Air		0.90
- In Argon		0.80

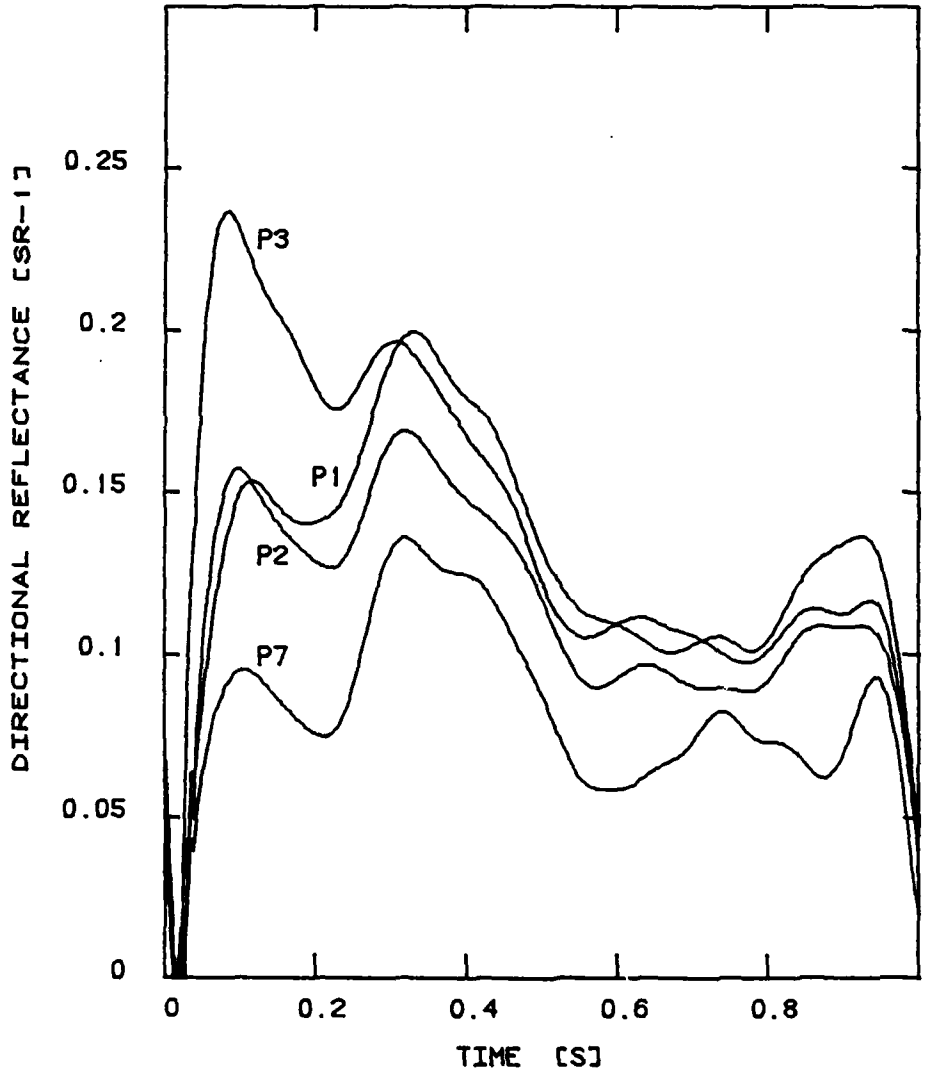

FIGURE 1 The directional reflectance (W sr^{-1} W^{-1}) of a GFRP sample in the direction of the array plates P1, P2, P3 and P7 (see text) as a function of irradiation time. The sample (GFRP 3) was irradiated at a power density of 60 MW m^{-2}.

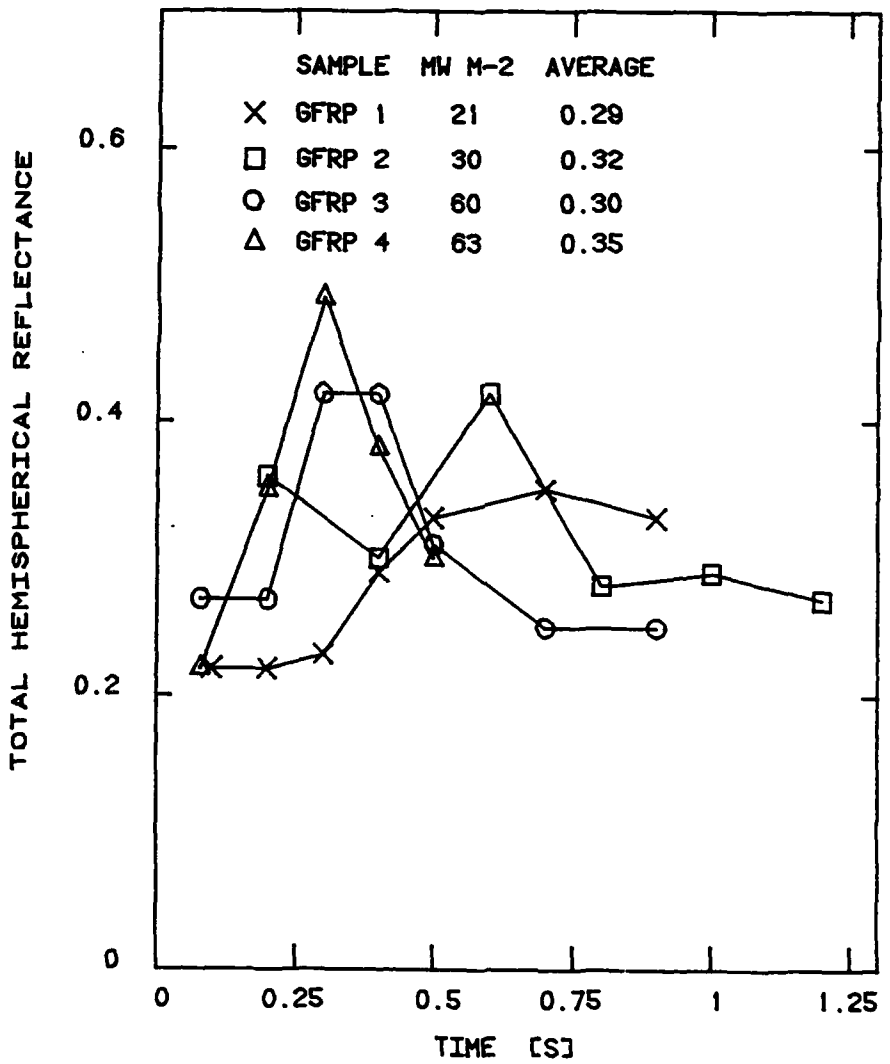

FIGURE 2 Total hemispherical reflectance as a function of time for GFRP samples irradiated at the power densities indicated. Also listed in the legend is the average value of the total hemispherical reflectance over the run time.

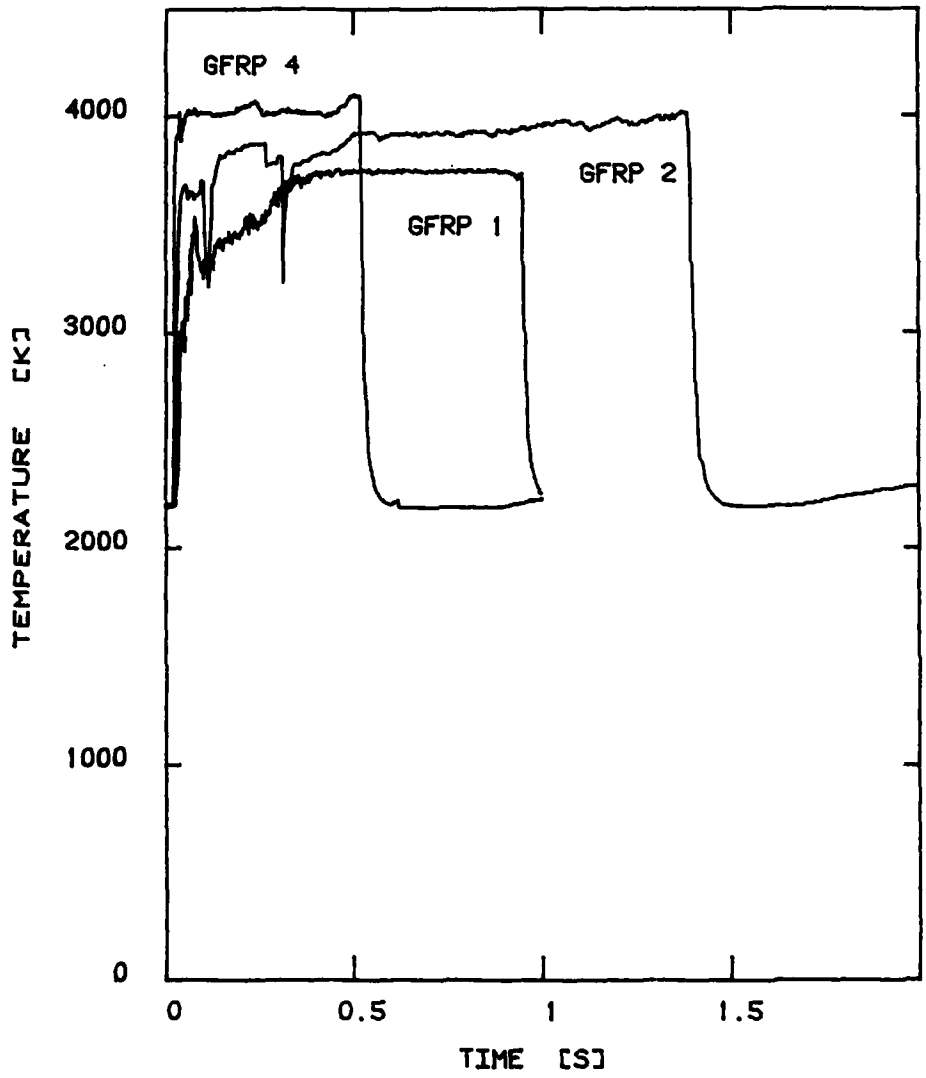

FIGURE 3 Surface temperature as a function of time for GFRP samples irradiated at power densities of about 21 MW m^{-2} (GFRP 1), 30 MW m^{-2} (GFRP 2) and 63 MW m^{-2} (GFRP 4).

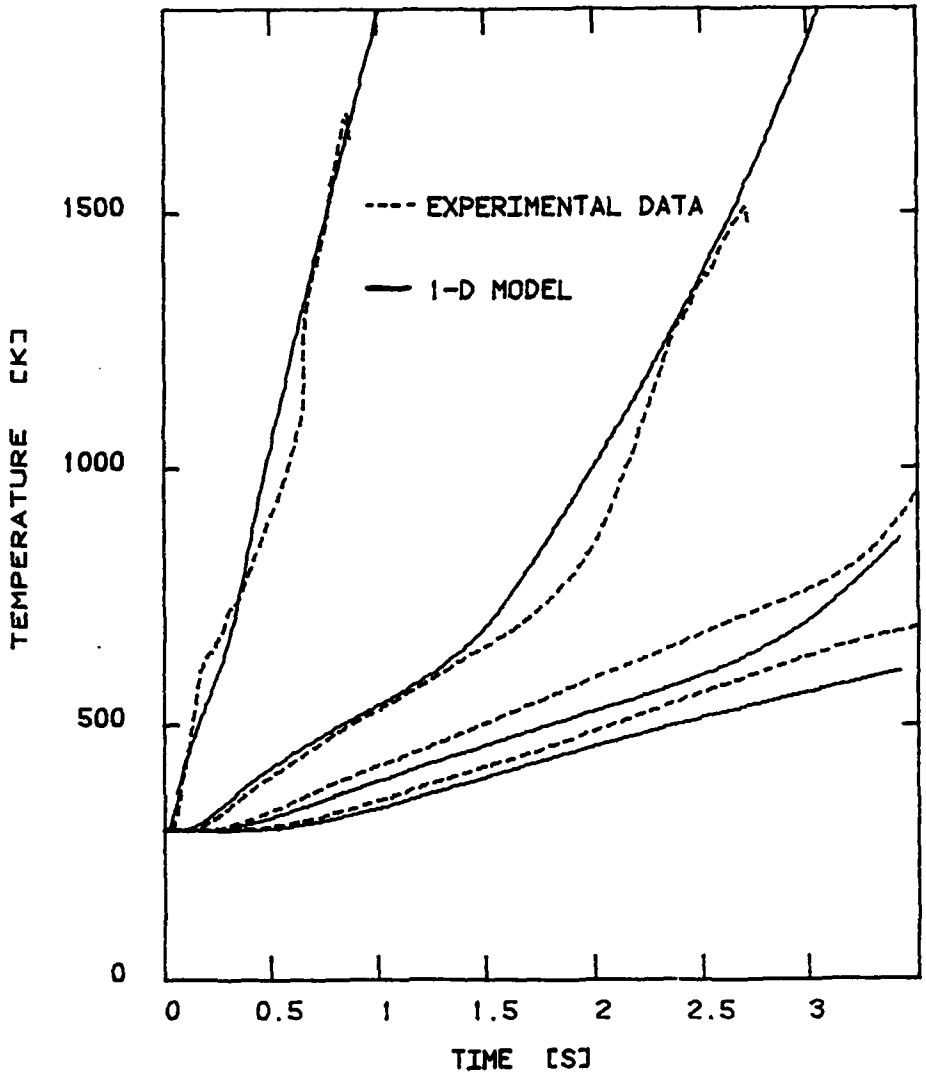

FIGURE 4 Temperatures in laser-irradiated GFRP material as a function of time for thermocouples located every second ply in an eight-ply sample. The target was irradiated at a power density of 21.3 kW/cm^2 in an air flow with M = 0.8. The solid lines are the temperatures predicted using the one-dimensional model of Griffis, Masumura and Chang [3].

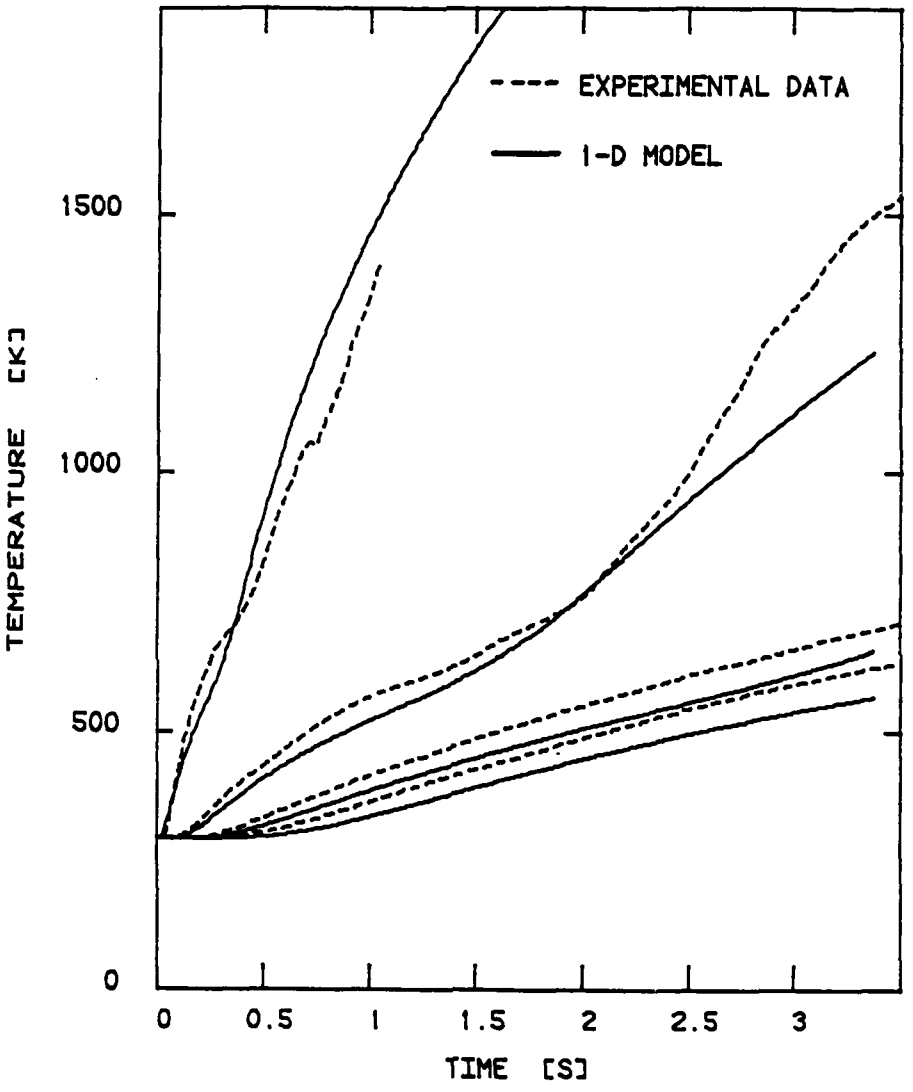

FIGURE 5 Temperatures in laser-irradiated GFRP material as a function of time for thermocouples located every second ply in an eight-ply sample. The target was irradiated at a power density of 17.2 kW/cm^2 in an argon flow with M = 0.6. The solid lines are the temperatures predicted using the one-dimensional model of Griffis, Masumura and Chang [3].

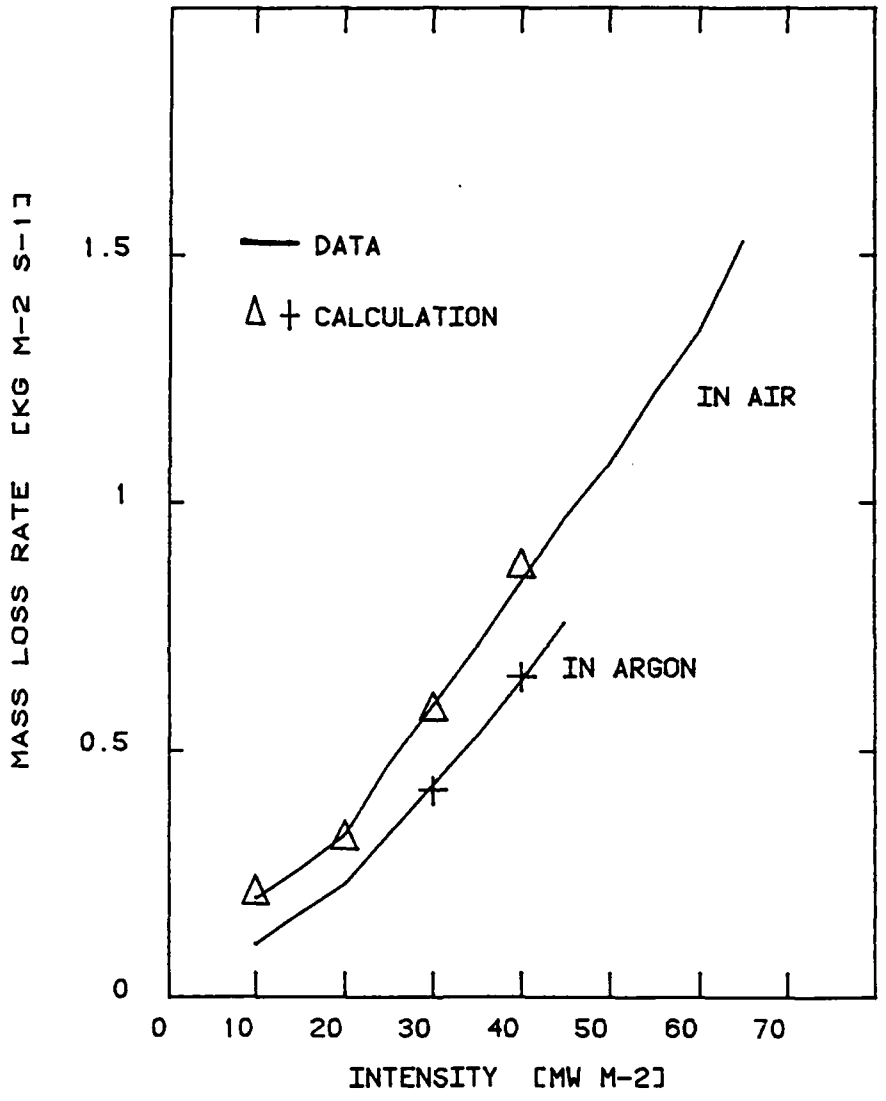

FIGURE 6 Mass-loss rate of GFRP material in air and in argon as a function of incident laser intensity. The solid line represents the data of Kennett and McLachlan [9]. The triangles and crosses are the results of calculations performed using the one-dimensional model of Griffis, Masumura and Chang [3].

END

DATE
FILMED

2-87

DTIC